Highly anisotropic magnetism in Cr-doped perovskite ruthenates

V. Durairaj, S. Chikara, X. N. Lin, A. Douglass, and G. Cao*
Department of Physics and Astronomy, University of Kentucky, Lexington, Kentucky 40506, USA

P. Schlottmann
Department of Physics, Florida State University, Tallahassee, Florida 32306, USA

E. S. Choi
National High Magnetic Field Laboratory, Florida State University, Tallahassee, Florida 32310, USA

R. P. Guertin
Department of Physics and Astronomy, Tufts University, Medford, Massachusetts 02155, USA
(Received 18 March 2006; published 8 June 2006)

Results of structural, magnetic and transport properties of single crystal $CaRu_{1-x}Cr_xO_3$ ($0 \leqslant x \leqslant 0.36$) and $SrRu_{1-x}Cr_xO_3$ ($0 \leqslant x \leqslant 0.20$) are reported. Cr substitution as low as $x=0.05$ drives $CaRu_{1-x}Cr_xO_3$ from the paramagnetic state to an itinerant ferromagnetic state with an abrupt jump in the isothermal magnetization leading to a sizeable saturation moment of 0.4 μ_B/f.u. aligned within the *ab* plane. The ferromagnetic behavior occurs abruptly and reaches a T_C as high as 123 K for $x=0.22$. The Cr-driven magnetism is highly anisotropic, suggesting an important role of the spin-orbit coupling in combination with the crystalline field states. Lattice constant and magnetic measurements strongly support the valence of Cr as tetravalent (Cr^{4+}, $3d^2$ configuration). Cr substitution for Ru in $SrRuO_3$ ($T_C=165$ K) enhances the itinerant ferromagnetism, consistent with Cr-induced ferromagnetism in paramagnetic $CaRuO_3$, but without significant magnetic anisotropy. All results indicate a coupling of Ru 4*d* and Cr 3*d* electrons that is unexpectedly favorable for itinerant ferromagnetism which often exists delicately in the ruthenates.

DOI: 10.1103/PhysRevB.73.214414 PACS number(s): 75.50.Cc, 71.30.+h, 75.30.−m

I. INTRODUCTION

The Ruddlesden-Popper (RP) series $Ca_{n+1}Ru_nO_{3n+1}$ and $Sr_{n+1}Ru_nO_{3n+1}$ (n=number of Ru-O layers/unit cell) are a class of correlated electron materials showing a rich variety of physical properties. The central characteristic of these 4*d*-shell based transition metal oxides is the more extended *d* orbitals of the Ru-ion as compared to those of 3*d*-shell ions. This leads to comparable and thus competing energies for the crystalline electric fields (CEF), Hund's rule interactions, spin-orbit coupling, *p-d* hybridization, and electron-lattice coupling. The deformations and relative orientations of corner-shared RuO_6 octahedra crucially determine the CEF level splitting, the band structure and hence the magnetic and transport properties. As a result, the physical properties are highly susceptible to perturbations such as applied magnetic fields, pressure and slight changes in chemical composition. These features are manifested in $Ca_{n+1}Ru_nO_{3n+1}$ and $Sr_{n+1}Ru_nO_{3n+1}$: The former are on the verge of a metal-nonmetal transition and prone to antiferromagnetism, whereas the latter are metallic and tend to be ferromagnetic with the *p*-wave superconductor Sr_2RuO_4 ($n=1$) being the exception.[1–32] Such a wide variety of physical properties has not been observed in other transition metal RP systems.

The perovskites $CaRuO_3$ and $SrRuO_3$ have been extensively studied (for example, Refs. 14–39) and their sharp differences in magnetic behavior are classic examples that illustrate the sensitivity of the band structure to structural distortions. Both compounds are orthorhombic, but $SrRuO_3$ has a more "ideal" (RP, $n=\infty$) and less distorted perovskite structure. $SrRuO_3$ is an itinerant ferromagnet with a Curie temperature $T_c=165$ K and a saturation moment M_s of 1.10 μ_B/Ru with the easy axis in the basal plane.[19] The CEF splitting in the Ru^{4+} ($4d^4$) ions is so large due to the extension of the 4*d* orbitals that Hund's rules partially break down, yielding a low spin state with $S=1$ ($^3T_{1g}$). On the other hand, $CaRuO_3$ forms in the same crystal structure and symmetry as $SrRuO_3$, but with a rotation of the RuO_6 octahedra approximately twice as large possibly due to ionic size mismatches between Ca and Ru ions (ionic radius $r=1.00$ Å and 1.18 Å for Ca^{2+} and Sr^{2+}, respectively, vs $r=0.620$ Å for Ru^{4+}). This yields a state less favorable for ferromagnetism, so that $CaRuO_3$ is a metallic paramagnet but verging on collective magnetism.[18,19,34–36] Our earlier study on single crystal $Sr_{1-x}Ca_xRuO_3$ indicates that the magnetic coupling is highly sensitive to perturbations to the Ru-O-Ru bond length and angle caused by substituting Sr with the isoelectronic smaller Ca-ion. As a result, T_c decreases monotonically with Ca concentration and vanishes for $x>0.8$ (Ref. 19). The sensitivity of the ground state to slight impurity doping is also evidenced in $CaRu_{1-x}Sn_xO_3$ (Ref. 18), $CaRu_{1-x}Rh_xO_3$ (Ref. 31), $SrRu_{1-x}Mn_xO_3$ (Ref. 32), $SrRu_{1-x}Pb_xO_3$ (Ref. 18), and other impurity doped $CaRuO_3$ (Ref. 36) and $SrRuO_3$ (Ref. 34), where substituting the Ru ions by the impurity ions extensively changes the magnetic ground state. This is often accompanied by a metal to insulator transition.

Cr ions substitute either in the trivalent ($3d^3$) or the tetravalent ($3d^2$) states. For Cr^{3+}, each of the three t_{2g} orbitals is half-filled, yielding $S=3/2$, while for the Cr^{4+} ion, only two of the three t_{2g} orbitals are singly occupied with the third

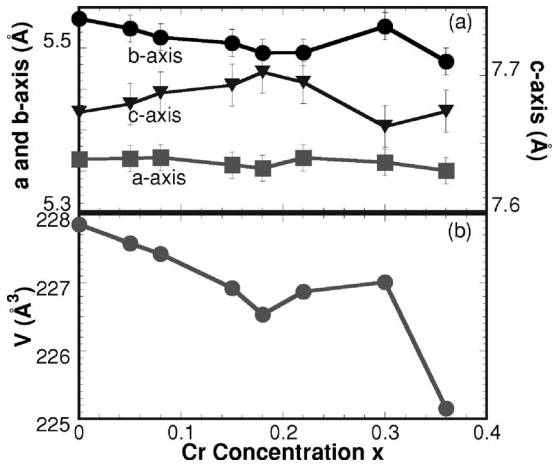

FIG. 1. (a) Lattice parameters for the a, b (left scale), and c axis (right scale) and (b) the volume of the unit V as a function of Cr concentration x for $CaRu_{1-x}Cr_xO_3$.

orbital empty, thus $S=1$. The perovskites $CaCrO_3$ and $SrCrO_3$, which form only under high pressure, were found to be an insulating antiferromagnet and a metallic paramagnet, respectively.[33] The difficulty with the synthesis still leaves many physical properties of these compounds largely unknown. $CaCrO_3$ has the same crystal structure and symmetry as $CaRuO_3$ with a space group of $Pbnm$ and lattice parameters $a=5.287$ Å, $b=5.316$ Å, and $c=7.486$ Å.[33] This structural compatibility, as shown in Fig. 1, provides an advantage for a thorough study of $CaRu_{1-x}Cr_xO_3$ by keeping the electron correlation strength without dramatically altering the onsite and intersite Coulomb interaction. On the other hand, $SrCrO_3$ has a cubic perovskite structure in the $Pm3m$ space group with $a=3.8169$ Å.[33] Recent studies on polycrystalline $SrRu_{1-x}Cr_xO_3$ show an increase in the Curie temperature T_C from 165 K for $x=0$ to 188 K for $x=0.11$ [Refs. 34, 35, and 39]. This behavior is attributed to a double-exchange interaction involving Cr^{3+} and Cr^{4+} [Refs. 35 and 39]. In contrast, all other transition metal substitutions for Ru rapidly diminish the Curie temperature. For instance, $SrRu_{1-x}Mn_xO_3$ displays an evolution through a quantum critical point from itinerant ferromagnetism to insulating antiferromagnetism with an increasing Mn concentration.[32]

In this paper, we report an abrupt transition from paramagnetism to itinerant ferromagnetism induced by Cr doping in single crystals of $CaRu_{1-x}Cr_xO_3$ with $0 \leqslant x \leqslant 0.36$. The itinerant ferromagnetism, with T_C as high as 123 K, occurs along with first-order metamagnetic transitions in the isothermal magnetization that lead to a saturation moment of 0.4 μ_B/f.u. aligned in the basal plane. The magnetic anisotropy in this orthorhombic system is unusually large, suggesting a critical role of the spin-orbit coupling that in conjunction with the large CEF splitting dominates the magnetic properties. Unlike other impurity doping on the Ru site, Cr doping essentially causes no metal-insulator transition for $x < 0.36$. As a comparison, we also present our recent results on single crystal $SrRu_{1-x}Cr_xO_3$ ($0 \leqslant x \leqslant 0.20$), where T_C rises from 165 to 290 K, consistent with results on polycrystalline samples published recently.[34,35,39] Unlike $CaRu_{1-x}Cr_xO_3$, $SrRu_{1-x}Cr_xO_3$ shows no significant magnetic anisotropy.

II. EXPERIMENT

Single crystals of the entire series of $CaRu_{1-x}Cr_xO_3$ and $SrRu_{1-x}Cr_xO_3$ were grown using flux techniques. All single crystals were grown in Pt crucibles from off-stoichiometric quantities of RuO_2, $CaCO_3$ ($SrCO_3$), and $CaCl_2$ ($SrCl_2$) mixtures with $CaCl_2$ ($SrCl_2$) being self-flux. The mixtures were first heated to 1430 °C in a Pt crucible covered by a Pt cover, soaked for 25 h, and slowly cooled at 2–3 °C/h to 1330 °C and finally cooled to room temperature at 100 °C/h. The starting Ca:Ru ratio and the thermal treatments are critical and subtle for the formation of perovskite crystals as nucleation of its sister compounds $(Ca,Sr)_3Ru_2O_7$ and $(Ca,Sr)_2RuO_4$ are also energetically favorable. By carefully changing the ratio and thermal treatments, we have successfully grown crystals of $Ca_{n+1}Ru_nO_{3n+1}$ and $Sr_{n+1}Ru_nO_{3n+1}$ with $n=1$, 2, 3, and ∞. The shape of the single crystals studied in this work is cubic. We used Lindberg box furnaces which provided high temperature stability critical for the crystal growth. All crystals studied were characterized by single crystal or powder x-ray diffraction, energy dispersive spectroscopy (EDS) and TEM. No impurities or intergrowth were found. The magnetization was measured using the Quantum Design MPMS XL 7T magnetometer. Since the shape of all crystals studied in this work are essentially cubic, the demagnetizing factor N for all three principal crystallographic axes is the same, and thus, the impact on magnetization M for the three orientations is expected to be the same. Including N in M in this case only slightly changes the slope of the isothermal magnetization $M(B)$ for the directions measured. The resistivity was obtained using the standard four-lead technique utilizing a transport property measurement option added to the magnetometer.

III. RESULTS

Shown in Fig. 1(a) are the lattice parameters for the a, b (left scale), and c axis (right scale) as a function of Cr concentration, x, ranging from 0 to 0.36 for $CaRu_{1-x}Cr_xO_3$. The lattice parameters are determined using x-ray diffraction data on powdered crystals. For $x=0$ ($CaRuO_3$), the lattice parameters are in good agreement with those reported earlier.[13,19] The orthorhombic symmetry is retained as a function of x. Within the error of the measurement, the lattice parameters generally decrease with x, consistent with the fact that the ionic radius of Cr^{4+} (0.550 Å) is smaller than that of Ru^{4+} (0.620 Å). The changes in the lattice parameters result in a shrinkage of the unit-cell volume by about 1.2% ($x=0.36$) as shown in Fig. 1(b). The results seem to suggest no existence of the Cr^{3+} ion (0.615 Å) and/or Ru^{5+} (0.565 Å), which would lead to x dependence opposite to that shown in Fig. 1. Similar changes in the lattice parameters are also observed in $SrRu_{1-x}Cr_xO_3$, consistent with those published.[39]

Shown in Fig. 2(a) is the temperature dependence of the a-axis magnetization, M_a, for representative compositions of $CaRu_{1-x}Cr_xO_3$ taken in a field cooled sequence. The major feature is that less than 5% of Cr doping is sufficient to induce ferromagnetic behavior. A strong hysteresis can be seen in the temperature dependence of M using field cooled

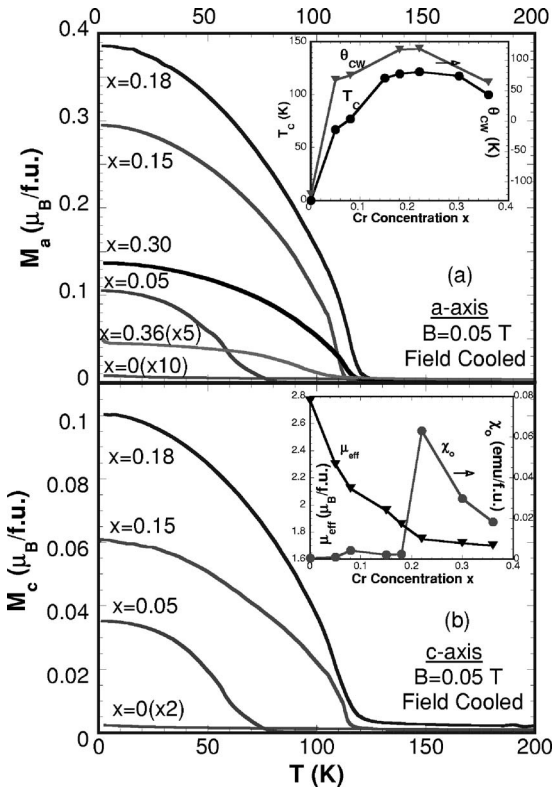

FIG. 2. (a) Temperature dependence of the *a*-axis magnetization *M* for representative compositions for $CaRu_{1-x}Cr_xO_3$; Inset: the Curie temperature T_c (left scale) and the Curie-Weiss temperature θ_{CW} (right scale) as a function of *x*. (b) Temperature dependence of the *c*-axis magnetization *M* for a few representative *x*; Inset: the effective moment μ_{eff} (left scale) and temperature-independent susceptibility χ_o (right scale) as a function of *x*.

and zero field cooled sequences (the zero field cooled data is not shown). The Curie temperature T_C increases from 67 K at $x=0.05$ to 115 K for $x=0.15$, peaks at 123 K for $0.18 \leqslant x \leqslant 0.22$ and decreases to 100 K for $x=0.36$ [see the inset of Fig. 2(a)]. Here T_C is determined as the maximum of the derivative dM/dT. The magnetic behavior is unexpectedly anisotropic as shown in Fig. 2(b) where the *c*-axis magnetization, M_c, is found much weaker than M_a. This anisotropy is stronger than expected, since the magnetization of the $x=0.0$ end compound, i.e., $CaRuO_3$, is much less anisotropic. It is noted that similar temperature dependence of *M* is seen in Ca_3LiRuO_6, which is known as a weak ferromagnet.[40]

The data for $200<T<350$ K and $0.00<x<0.36$ in Fig. 2 were fitted to a Curie-Weiss law $\chi=\chi_o+C/(T-\theta_{CW})$, where χ_o is a temperature-independent susceptibility, *C* is the Curie constant, and θ_{CW} the Curie-Weiss temperature. In the paramagnetic phase the susceptibility is essentially isotropic, so that the susceptibilities with the field along the *a* or *c* axis yield the same parameters. Remarkably, the Curie-Weiss temperature θ_{CW} shows an *x* dependence parallel to that of T_c, changing from −150 K for $x=0.0$ through zero at very small *x* (less than 5% Cr) to +120 K for maximum T_c [see the inset in Fig. 2(a)]. The change in sign is associated with the change from antiferromagnetic to ferromagnetic exchange correlations and is consistent with the occurrence of the ferromagnetism with increasing *x*.

The effective moment estimated from the Curie constant *C* varies monotonically from 2.76 μ_B/f.u. for $x=0$ to 1.7 μ_B/f.u. for $x=0.36$ [see the inset in Fig. 2(b)]. These values are smaller but close to those anticipated for tetravalent Ru and Cr ions, i.e., $S=1$ for both Ru^{4+} ($4d^4$, low spin state) and Cr^{4+} ($3d^2$). Note that the effective magnetic moments for Ru^{5+} ($S=3/2$) and Cr^{3+} ($S=3/2$) are considerably larger, so that the Curie constant is only consistent with tetravalent Ru and Cr ions for all compositions. The results are in agreement with the structural data shown in Fig. 1. Also illustrated in the inset in Fig. 2(b) is the temperature-independent susceptibility χ_o (right scale) which stays essentially unchanged for $x<0.18$, but rises rapidly near $x=0.18$ and peaks at $x=0.22$ where T_C reaches the maximum. χ_o is usually associated with a Pauli susceptibility and a measure of the density of (localized and itinerant) states at the Fermi level, $N(\varepsilon)$, i.e., $\chi_o \sim N(\varepsilon)$, so that the rapid increase of χ_o can then be attributed to an increase of the density of the states.

Figure 3 shows the isothermal magnetization for both the *a* axis [Fig. 3(a)] and *c* axis [Fig. 3(b)] at $T=2$ K. $M(B)$ was obtained by first cooling the sample in zero field from $T>T_C$ to the target temperature (e.g., $T=2$ K), and then sweeping the field up and down. This sequence was repeated for all other temperatures. The striking behavior is the abrupt transition with strong hysteresis for M_a starting at $x=0.05$ [Fig. 3(a)]. This transition then develops into a two-step transition for $x=0.15$ and 0.18. As shown in Fig. 3(c), this two-step transition for $x=0.15$ sensitively depends on the temperature and vanishes near 50 K. However, the magnitude of *M* shows only a weak dependence on temperature. In addition, for the *a* axis, the ordered moment, M_s, obtained by extrapolating *M* to zero-field $B=0$, increases initially with *x* from 0 for $x=0$ to 0.4 μ_B for $x=0.18$, and then it decreases for $x>0.18$ as seen in Fig. 3(e). In contrast, M_s for the *c* axis is much smaller [see Fig. 3(b)]. This suggests that the interplay of crystalline fields with the spin-orbit coupling is the cause of the anisotropy. Figure 3(d) clearly shows this anisotropy between the *a*, *b*, and *c* axis. It is apparent that the two-step transition is a unique property of the *a* axis. The anisotropy of $M(B)$ for the *a* and *b* axis confirms that the crystals are indeed untwined single crystals. It is noted that the variations of both χ_o and M_s are larger in the vicinity of $x=0.18$, implying an intimate correlation between the density of states and the ordered moment. In addition, the linear field dependence of *M* below the transition may suggest the presence of an antiferromagnetic component.

Although the low temperature resistivity also undergoes significant changes with *x*, the metallic behavior essentially remains for all *x* except for $x=0.36$. As seen in Fig. 4, the *ab*-plane resistivity, ρ_{ab} for $T<100$ K rises and becomes less temperature dependent with increasing *x*. Nevertheless, ρ_{ab}, on a logarithmic scale as a function of temperature varies by less than two orders of magnitude from $x=0$ to $x=0.36$ at 2 K. ρ_{ab} for $x=0$ and 0.08 obey $\rho=\rho_o+AT^2$ (ρ_o is the residual resistivity and *A* the Fermi liquid coefficient) for $T<40$ K. ρ_o is 18 and 115 $\mu\Omega$ cm whereas *A* is 45 and 3.4 10^{-9} Ω cm K^{-2}, for $x=0$ and 0.08, respectively. An increase in ρ_o is expected for any impurity doping that causes more

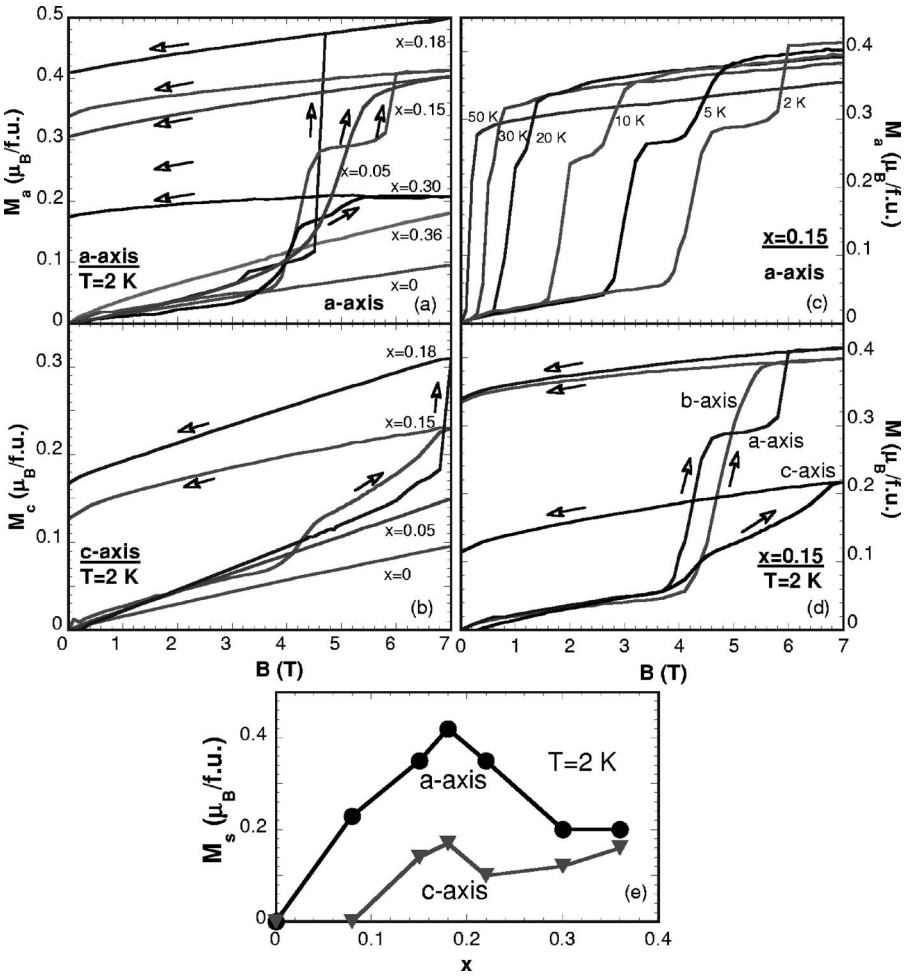

FIG. 3. (a) Isothermal magnetization $M(B)$ for the a axis at $T=2$ K $CaRu_{1-x}Cr_xO_3$; (b) $M(B)$ for the c axis at $T=2$ K; (c) $M(B)$ for $x=0.15$ for various temperatures; (d) $M(B)$ for $x=0.15$ for a, b, and c axis; (e) Saturation moment M_s as function of x for both the a and c axis.

elastic scattering. The coefficient A is proportional to the square of the effective mass, m^*, i.e., $A \sim m^{*2}$. The value of A is comparable to those of other correlated electron systems with moderate mass enhancement. At $x=0.36$, ρ_{ab} shows brief nonmetallic behavior below 20 K and a sharp break in the slope at $T_C=100$ K [see the inset in Fig. 4], which according to the Fisher-Langer theory is the consequence of scattering off short-range spin fluctuations in the neighborhood of T_C. It is noted that the Fisher-Langer behavior for other concentrations is not as strong as that for $x=0.36$. Finally, the largest negative magnetoresistence ratio, estimated from ρ_{ab} as a function of B, occurs at low temperatures. For $x=0.18$, the ratio is about 20% for $T=2$ K and $B=7$ T.

The results discussed above for $CaRu_{1-x}Cr_xO_3$ are supported by a parallel study on $SrRu_{1-x}Cr_xO_3$ showing that Cr doping significantly raises the Curie temperature—from $T_C=165$ K for $x=0$ to $T_C=192$ K for $x=0.20$, as shown in Fig. 5(a). The values of T_C are consistent with those of polycrystalline samples reported earlier.[34,35,39] It is worth mentioning that T_C becomes as high as 290 K for a larger x though T_C is largely broadened (not shown, to be published elsewhere with results for heavily Cr doped $SrRuO_3$). The field dependence of the magnetization stays essentially unchanged for all x, but the saturation moment M_s decreases with increasing x. M_s is reduced from 1.1 μ_B/f.u. for $x=0$ to 0.50 μ_B/f.u. for $x=0.20$ [see Fig. 5(c)]. All samples remain metallic and display a sharp decrease at T_C, suggesting a significant reduction of spin scattering as displayed in Fig. 5(b). A noticeable difference between $SrRu_{1-x}Cr_xO_3$ and $CaRu_{1-x}Cr_xO_3$ is that the latter is characterized by the extraordinarily large magnetic anisotropy whereas the former is essentially magnetically isotropic. This different behavior, which is somewhat unexpected, reflects the different ionic radii of Sr^{2+} and

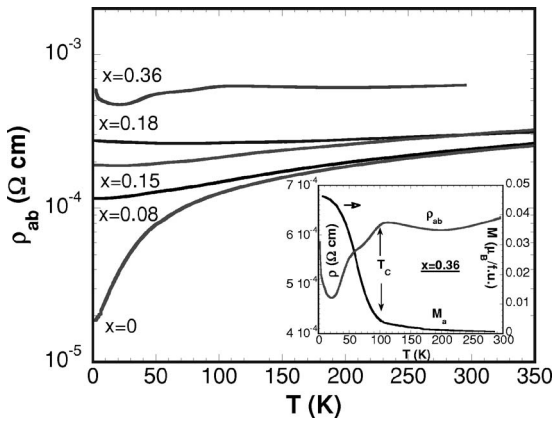

FIG. 4. (a) Basal plane resistivity ρ_{ab} on a logarithmic scale vs temperature for $x=0$, 0.08, 0.15, 0.18, and 0.36; Inset: ρ_{ab} (left scale) and M (right scale) as a function of temperature for $x=0.36$.

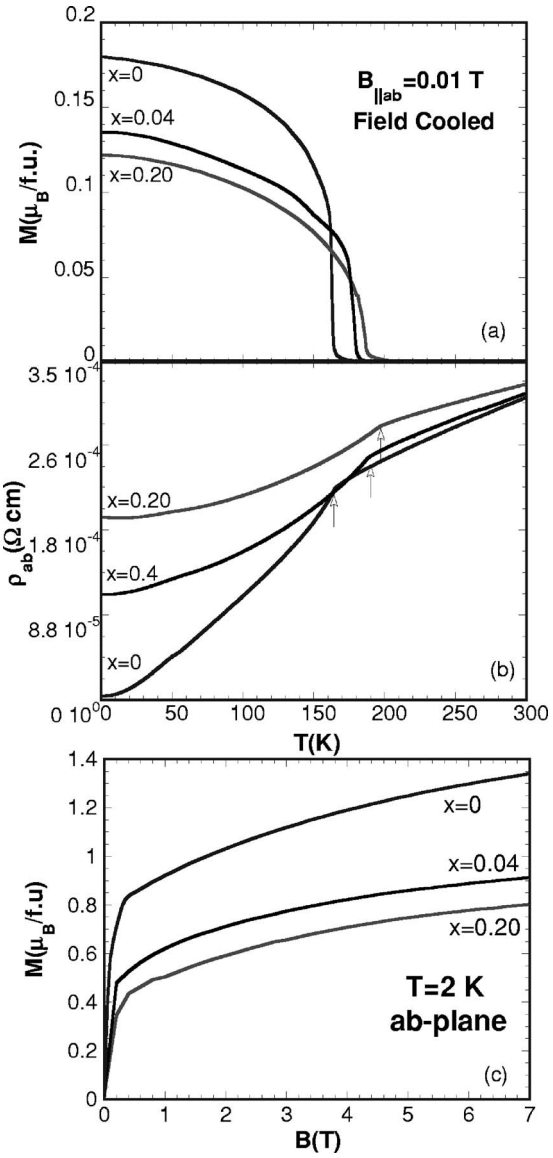

FIG. 5. (a) Temperature dependence of (a) the *a*-axis magnetization M and (b) the *ab*-plane resistivity ρ_{ab} for $SrRu_{1-x}Cr_xO_3$ for $x=0$, 0.04, and 0.2; (c) Isothermal magnetization M for the *ab* plane at $T=2$ K.

Ca^{2+} and the concomitant different CEF splitting of the Ru^{4+} levels.

In addition, the magnetization $M(B)$ using an anvil pressure cell was also performed at $P\sim4$ kbar and $P\sim7$ kbar for $x=0.15$ of $CaRu_{1-x}Cr_xO_3$. While little shift was seen in the position of the transition or in the Curie temperature, a very large overall increase in $M(B)$ was observed, attaining a 25% increase for $P\sim7$ kbar. The result is in contrast, for example, to the $T_c(P)$ for MnSi, a weak itinerant ferromagnet, where $T_C\sim(\text{Pc-}P)^{1/2}$, a prediction of Stoner theory. Decreasing the lattice constant in ferromagnetic $CaRu_{1-x}Cr_xO_3$ or enhancing the buckling of octahedral RuO_6 may reduce the overlap of the t_{2g} orbitals and, hence, increase the moment through band narrowing, but it seems not to strongly affect T_c. This effect deserves further study.

IV. DISCUSSION

Low levels of substitution of Ru t_{2g} electrons by Cr t_{2g} electrons induces ferromagnetism and metamagnetism. In $CaRuO_3$, the $4d$ t_{2g}-orbitals are itinerant due to self-doping by the O $2p$ electrons and the system is metallic. On the other hand, Cr^{4+}-ion based compounds have two $3d$ electrons in more contracted t_{2g} orbitals, which should provide both a fairly narrow band and strong exchange interactions between the electrons. This is certainly true for CrO_2, an itinerant half-metallic ferromagnet with $T_C=400$ K, where the exchange splitting between spin-up and spin-down electrons is comparable to the t_{2g} bandwidth, that makes a 100% spin polarization possible. The substitution of Ru^{4+} by Cr^{4+} replaces four $4d$ electrons with two $3d$ electrons, both ions with a total spin-one configuration. The mismatch between the energy levels and the symmetries of the wave functions reduces the effective hybridization and narrows the effective bandwidth W. This may also give rise to localization of d electrons. A significant local reduction in W may enhance the density of states enough $[W\sim1/N(\varepsilon)]$, so that according to the Stoner model ferromagnetism may occur. Furthermore, ferromagnetism may also be induced if $N(\varepsilon)$ has a sharp peak close to the Fermi level. The Stoner criterion for the ferromagnetic instability, $U_cN(\varepsilon)=1$, may be satisfied upon doping with holes as a function of x. Here U_c is the critical value of the exchange interaction.

T_C and θ_{CW} are maximum at about $x=0.20$, and also χ_o (proportional to the density of states) and M_s are maximum around $x=0.20$. This concentration is much less than expected from nearest neighbor site percolation of bonds ($x_c\sim0.307$), but larger than for nearest and next-to-nearest neighbor site percolation of bonds ($x_c\sim0.137$). This could be an indication that bonds are not just "on or off," but that there is a distribution of bond strengths.

Unlike other $3d$ impurity doping in $SrRuO_3$, which reduce T_C, the Ru $4d$ electrons and the Cr $3d$ electrons are strikingly synergetic, leading to a highly enhanced exchange interaction and/or narrowed bandwidth favorable for ferromagnetism. This is particularly unusual for the perovskite ruthenates as ferromagnetism exists only in a structure that allows no significant distortions of Ru-O-Ru bonds and angles.[20] Also largely unexpected are the abrupt transitions in $M(B)$ for $CaRu_{1-x}Cr_xO_3$, which seemingly suggest a metamagnetic transition rather than movements of domains. But metamagnetism is only expected to occur in an enhanced paramagnetic or a nearly ferromagnetic state that is characterized by a broad maximum in the magnetic susceptibility,[41] which is not observed in $CaRu_{1-x}Cr_xO_3$. On the other hand, the transitions observed might be too abrupt to be due to domain movement, which is usually a gradual development. Furthermore, the two-step transition seen in $M(B)$ for $x=0.08$, 0.15, and 0.18 is not characteristic of ordinary domain wall motion. This issue, which is interesting and yet puzzling, is yet to be understood. No metamagnetic transition is discerned in $SrRu_{1-x}Cr_xO_3$ (see Fig. 5).

In the ruthenates the transport properties, like the magnetic properties, strongly depend on the relative orientation

of the corner-shared octahedra, and there is a strong coupling of lattice, charge, orbital, and spin degrees of freedom. The drastic changes in magnetic behavior in $CaRu_{1-x}Cr_xO_3$ and $SrRu_{1-x}Cr_xO_3$ with Cr doping conspicuously accompany a no metal-insulator transition that is often observed for other impurity doping.[18,31,32,36] This may be again associated with the fact that only two of three Cr t_{2g} levels are occupied, and electron hopping between the t_{2g} orbitals is still energetically possible, so the itinerant character and dynamics of the *d* electrons are retained. Of course, the impurity doping introduces defects and disorder raising the electrical resistivity at low temperatures. The less metallic behavior for large *x* could be also associated with a site percolation of nearest neighbor Ru-Ru bonds.[42] The disruption of Ru connectivity affects the orientation of the RuO_6 octahedra (tilting angle), which to a great extent determines the properties of the ruthenates. A reduced connectivity tends to localize the electrons and leads to an increased density of states at the Fermi level.

V. CONCLUSIONS

Unlike all other impurity doping for the Ru site, slight Cr doping facilitates the presence of the ferromagnetism that is extremely delicate in the perovskite ruthenates. The same effect is also seen in the triple layered $Sr_4Ru_3O_{10}$ [Ref. 43]. Apparently, the Ru 4*d* electrons and Cr 3*d* electrons are unusually synergistic to promote ferromagnetism in these materials. The phenomena merit additional experimental and theoretical investigations.

ACKNOWLEDGMENTS

G.C. is indebted to Joseph Budnick for valuable discussions that resulted in this work. This work was supported by National Science Foundation under Grants No. DMR-0240813 and No. DMR-0400938. P.S. acknowledges the support by DOE under Grant No. DE-FG02-98ER45707. R.P.G. acknowledges the support of the National High Magnetic Field Laboratory under Grant No. VSP#43.

*Email address: cao@uky.edu

[1] X. N. Lin, Z. X. Zhou, V. Durairaj, P. Schlottmann, and G. Cao, Phys. Rev. Lett. **95**, 017203 (2005).
[2] Y. Maeno, T. M. Rice, and M. Sigrist, Phys. Today **54**, 42 (2001).
[3] Y. Maeno, H. Hashingmoto, K. Yoshida, S. Ishizaki, T. Fujita, J. G. Bednorz, and F. Lichtenberg, Nature (London) **372**, 532 (1994).
[4] G. Cao, S McCall, M. Shepard, J. E. Crow, and R. P. Guertin, Phys. Rev. B **56**, R2916 (1997).
[5] C. S. Alexander, G. Cao, V. Dobrosavljevic, S. McCall, J. E. Crow, E. Lochner, and R. P. Guertin, Phys. Rev. B **60**, R8422 (1999).
[6] G. Cao, S. McCall, J. E. Crow, and R. P. Guertin, Phys. Rev. Lett. **78**, 1751 (1997).
[7] A. V. Puchkov, M. C. Schabel, D. N. Basov, T. Startseva, G. Cao, T. Timusk, and Z.-X. Shen, Phys. Rev. Lett. **81**, 2747 (1998).
[8] G. Cao, L. Balicas, Y. Xin, E. Dagotto, J. E. Crow, C. S. Nelson, and D. F. Agterberg, Phys. Rev. B **67**, 060406(R) (2003).
[9] G. Cao, L. Balicas, X. N. Lin, S. Chikara, E. Elhami, V. Durairaj, J. W. Brill, and R. C. Rai, Phys. Rev. B **69**, 014404 (2004).
[10] S. A. Grigera, R. S. Perry, A. J. Schofield, M. Chiao, S. R. Julian, G. G. Lonzarich, S. I. Ikeda, Y. Maeno, A. J. Millis, and A. P. Mackenzie, Science **294**, 329 (2001).
[11] G. Cao, L. Balicas, W. H. Song, Y. P. Sun, Y. Xin, V. A. Bondarenko, J. W. Brill, S. Parkin, and X. N. Lin, Phys. Rev. B **68**, 174409 (2003).
[12] M. K. Crawford, R. L. Harlow, W. Marshall, Z. Li, G. Cao, R. L. Lindstrom, Q. Huang, and J. W. Lynn, Phys. Rev. B **65**, 214412 (2002).
[13] J. J. Randall and R. Ward, J. Am. Chem. Soc. **81**, 2629 (1959).
[14] R. A. Rao, Q. Gan, and C. B. Eom, Appl. Phys. Lett. **71**, 1171 (1997).
[15] P. B. Allen, H. Berger, O. Chauvet, L. Forro, T. Jarlborg, A. Junod, B. Revaz, and G. Santi, Phys. Rev. B **53**, 4393 (1996).
[16] L. Klein, J. S. Dodge, C. H. Ahn, G. J. Snyder, T. H. Geballe, M. R. Beasley, and A. Kapitulnik, Phys. Rev. Lett. **77**, 2774 (1996).
[17] L. Klein, J. R. Reiner, T. H. Geballe, M. R. Beasley, and A. Kapitulnik, Phys. Rev. B **61**, R7842 (2000).
[18] G. Cao, S. McCall, J. Bolivar, M. Shepard, F. Freibert, P. Henning, J. E. Crow, and T. Yuen, Phys. Rev. B **54**, 15144 (1996).
[19] G. Cao, S. McCall, M. Shepard, J. E. Crow, and R. P. Guertin, Phys. Rev. B **56**, 321 (1997).
[20] I. I. Mazin and D. J. Singh, Phys. Rev. B **56**, 2556 (1997).
[21] K. Fujioka, J. Okamoto, T. Mizokawa, A. Fujimori, I. Hase, M. Abbate, H. J. Lin, C. T. Chen, Y. Takeda, and M. Takano, Phys. Rev. B **56**, 6380 (1997).
[22] L. Klein, J. R. Reiner, T. H. Geballe, M. R. Beasley, and A. Kapitulnik, Phys. Rev. B **61**, R7842 (2000).
[23] A. P. Mackenzie, J. W. Reiner, A. W. Tyler, L. M. Galvin, S. R. Julian, M. R. Beasley, T. H. Geballe, and A. Kapitulnik, Phys. Rev. B **58**, R13318 (1998).
[24] P. Kostic, Y. Okada, N. C. Collins, Z. Schlesinger, J. W. Reiner, L. Klein, A. Kapitulnik, T. H. Geballe, and M. R. Beasley, Phys. Rev. Lett. **81**, 2498 (1998).
[25] M. S. Laad and E. Müller-Hartmann, Phys. Rev. Lett. **87**, 246402 (2001).
[26] L. Capogna, A. P. Mackenzie, R. S. Perry, S. A. Grigera, L. M. Galvin, P. Raychaudhuri, A. J. Schofield, C. S. Alexander, G. Cao, S. R. Julian, and Y. Maeno, Phys. Rev. Lett. **88**, 076602 (2002).
[27] D. Kim, B. L. Zink, F. Hellman, S. McCall, G. Cao, and J. E. Crow, Phys. Rev. B **67**, 100406(R) (2003).
[28] G. Cao, W. H. Song, Y. P. Sun, and X. N. Lin, Solid State Commun. **131**, 331 (2004).
[29] C. S. Alexander, S. McCall, P. Schlottmann, J. E. Crow, and G. Cao, Phys. Rev. B **72**, 024415 (2005).
[30] G. Cao, Y. Xin, C. S. Alexander, and J. E. Crow, Phys. Rev. B **63**, 184432 (2001).
[31] G. Cao, F. Freibert, and J. E. Crow, J. Appl. Phys. **81**, 3884 (1997).
[32] G. Cao, S. Chikara, X. N. Lin, E. Elhami, V. Dufairaj, and P. Schlottmann, Phys. Rev. B **71**, 035104 (2005).

[33] J. B. Goodenough, J. M. Longo, and J. A. Kafalas, Mater. Res. Bull. **3**, 471 (1968).
[34] L. Pi, A. Maignan, R. Retoux, and B. Raveau, J. Phys.: Condens. Matter **14**, 7391 (2002).
[35] Z. H. Han, J. I. Budnick, W. A. Hines, B. Dabrowski, S. Kolesnik, and T. Maxwell, J. Phys.: Condens. Matter **17**, 1193 (2005).
[36] T. He and R. J. Cava, J. Phys.: Condens. Matter **13**, 8347 (2001).
[37] B. Dabrowski, O. Chmaissem, P. W. Klamut, S. Kolesnik, M. Maxwell, J. Mais, Y. Ito, B. D. Armstrong, J. D. Jorgensen, and S. Short, Phys. Rev. B **70**, 014423 (2004).
[38] B. Dabrowski, M. Andreev, O. Chmaissem, S. Kolesnik, P. W. Klamut, M. Maxwell, M. Avdeev, and J. D. Jorgensen, Phys. Rev. B **71**, 104411 (2005).
[39] B. Dabrowski, S. Kolesnik, O. Chmaissem, T. Maxwell, M. Avdeev, P. W. Barnes, and J. D. Jorgensen, Phys. Rev. B **72**, 054428 (2005).
[40] P. L. Paulose, M. M. Kumar, S. Mazumdar, and E. V. Sampathkumaran, J. Phys.: Condens. Matter **12**, 8889 (2000).
[41] E. P. Wohlfarth and P. Rhodes, Philos. Mag. **7**, 1817 (1962).
[42] J. W. Essam, in *Phase Transitions and Critical Phenomena*, edited by C. Domb and M. S. Green (Academic Press, London, 1972), Vol. 2, p. 197.
[43] S. Chikara *et al.* (unpublished).